inorganics

MDPI

Article

Nanostructured γ-Al_2O_3 Synthesis Using an Arc Discharge Method and its Application as an Antibacterial Agent against XDR Bacteria

Awatif Rashed Z. Almotairy [1], A. M. Amer [2], Hadir El-Kady [3], Bassma H. Elwakil [3,*], Mostafa El-Khatib [4] and Ahmed M. Eldrieny [5]

[1] Department of Chemistry, Faculty of Science, Taibah University, Yanbu 30799, Saudi Arabia
[2] College of Engineering and Technology, American University of the Middle East, Egaila 54200, Kuwait
[3] Department of Medical Laboratory Technology, Faculty of Applied Health Sciences Technology, Pharos University in Alexandria, Alexandria 21500, Egypt
[4] Department of Basic Sciences, Faculty of Engineering, Pharos University in Alexandria, Alexandria 21500, Egypt
[5] Department of Radiological Imaging, Faculty of Applied Health Sciences Technology, Pharos University in Alexandria, Alexandria 21500, Egypt
* Correspondence: bassma.hassan@pua.edu.eg

Abstract: In the last few years, many efforts have been devoted to investigating the antibacterial activity of metal nanoparticles, especially against multidrug-resistant bacteria. Recently extensively drug-resistant (XDR) bacteria have emerged and caused a global threat. The purpose of this manuscript was to synthesize nanostructured γ-Al_2O_3 as an antibacterial agent against some XDRs. The results showed that Al_2O_3 was a mix of rod and spherical shapes in the nano range with diameters of less than 30 nm. The zeta potential was determined to estimate the surface charge for the synthesized γ-Al_2O_3, which was recorded as -34 ± 1.8 mV, indicating good stability. The synthesized nanostructured γ-Al_2O_3 showed a potent antibacterial activity against extensively drug-resistant *Acinetobacter baumanii*, with an inhibition zone diameter that reached 19 mm and a minimum inhibitory concentration (MIC) value that reached 2 µg/mL. The observed antibacterial activity of the prepared Al_2O_3 nanoparticles confirmed that the main mechanistic actions include bacterial cells apoptosis, ROS increment, cellular membrane disruption, and DNA damage. The cytotoxic effect (CC50) of the prepared γ-Al_2O_3-NPs was 1250 µg/mL in a normal human lung fibroblast cell line (WI-38 cells). It can be concluded that the synthesized γ-Al_2O_3 had an acceptable toxicity, which may pave the way for its use as a potent agent in the fight against XDR bacteria.

Keywords: arc discharge; aluminum oxides; antibacterial activity; extensively drug-resistant bacteria

Citation: Almotairy, A.R.Z.; Amer, A.M.; El-Kady, H.; Elwakil, B.H.; El-Khatib, M.; Eldrieny, A.M. Nanostructured γ-Al_2O_3 Synthesis Using an Arc Discharge Method and its Application as an Antibacterial Agent against XDR Bacteria. *Inorganics* **2023**, *11*, 42. https://doi.org/10.3390/inorganics11010042

Academic Editor: Arthur D. Tinoco

Received: 23 November 2022
Revised: 30 December 2022
Accepted: 3 January 2023
Published: 15 January 2023

1. Introduction

It is critical to investigate the uses of produced nanoparticles in tackling certain severe problems such as the emerging need to synthesize antibacterial substances against some critical illnesses [1]. To address these issues, there is a quest for a new generation of materials that can effectively combat bacterial infections with very low cell toxicity [2]. In the last era, arc discharge machines were used as an ecofriendly physical method to prepare nanometals without using toxic chemicals [3,4]. The arc discharge method was first utilized by Iijima in 1991 to fabricate carbon nanotubes [5]. Methods for the preparation of nanomaterials have been expanded over the decades, showing that the shapes, sizes and phase structures are strongly dependent on the arc discharge parameters, e.g., temperature, current, voltage, type of power supply, pressure, dielectric media, electrode shape, and the gap between the metallic electrodes [6]. Aluminum oxide nanoparticles (AlOxNPs) were obtained in three main forms: spherical, rod-like, and flake-like. Nanomaterials with various architectures, particularly the construction, size, and anisotropy, offer significant promise for bacterial

inhibition. However, recent studies have reported the limitation of superhydrophobic surfaces in controlling bacterial infections, such as alumina [7,8]. Researchers focused on nanoparticle research and applications because of the unusual characteristics of Al_2O_3 [9]. However, a strong electric field is required to break the potential barrier (dielectric medium) that separates the electrodes for the arc discharge method to be successful. A strong electric field causes electron emission, producing ions; this is known as the Schottky effect [10]. The most important benefit of applying metal oxide nanoparticles in the biomedical industry (as antimicrobial agents) is their observed effectiveness, even against superbugs (antibiotic-resistant strains). Delaportas et al. [11] and Li et al. [12] successfully synthesized γ-Al_2O_3 using DC electric arc discharge. In the past 10 years, Al_2O_3-NPs have been employed successfully as an antibacterial agent [13]. Even at low dosages, Al_2O_3-NPs have effective antibacterial actions against numerous harmful microorganisms and effectively produce full growth suppression of microorganisms. Al_2O_3-NPs have been identified as potent inhibitors of antibiotic-resistant bacteria [14].

The public health community refers to multidrug-resistant organisms (MDROs) as superbugs with relatively few available treatments. Only one or two antibiotics (with hazardous side effects) may be successful against some MDROs. Boucher et al. [15] described ESKAPE organisms as "Bad Bugs" in 2009, where the E stands for *Enterococcus faecium*, S stands for *Staphylococcus aureus*, K stands for *Klebsiella pneumoniae*, A stands for *Acinetobacter baumannii*, P stands for *Pseudomonas aeruginosa*, and E stands for *Enterobacter* species [15]. Infectious illness rates have risen so dramatically over the past two decades that in many areas of the world public health is already approaching pre-antibiotic levels [16]. The terms "multidrug-resistant" (MDR), "extensively drug-resistant" (XDR), and "pan drug-resistant" (PDR) bacteria have been defined in accordance with standardized international terminology developed by the European Centre for Disease Control (ECDC) and the Centers for Disease Control and Prevention (CDC) [17]. Extensively drug-resistant (XDR) was defined as the inability of a bacterial isolate to be sensitive to more than one agent in any but two or fewer antimicrobial groups [18].

To the best of our knowledge, very limited information is available about the antibacterial activity of Al_2O_3-NPs against XDR bacteria. Hence, in the present investigation, we aimed to synthesize Al_2O_3 nanoparticles (NPs) through an arc discharge method and conduct in vitro investigations of their antimicrobial activity against extensively drug-resistant strains of *Acinetobacter baumannii*.

2. Materials and Methods

2.1. Nanoparticle Synthesis

High-purity γ-Al_2O_3 was synthesized using the arc discharge method by using a pure cathodic aluminum electrode with a diameter of 16 mm and a length of 10 cm with an aluminum anode with a diameter of 2 mm and a length of 3 cm. The alternating current was fixed at 15 A, a voltage of 70 was used, the vessel capacity was 3 liters, the rotational speed was 950 rpm, and the experiment was carried out under atmospheric pressure. The pH was adjusted using HCl drops to reach 5, and the electrode gap was about 0.5 mm in deionized water to synthesize the γ-Al_2O_3, as designed [19].

2.2. Filtration and Characterization

Filtration was performed using a refrigerated ultracentrifuge (Hettich MIKRO, Germany), and the nanoparticles separation carried out according to their mass, where the precipitated part contained the solid particles. The relative centrifugal force (RCF) was then calculated using Equation (1) [20]:

$$RCF = 1.118 \times 10^{-5} \times r \times N^2 \quad (1)$$

where RCF is the relative centrifugal force (cm/s^2), r is the rotational radius (cm), and N is the rotating speed (revolutions per minute, rpm). Then, each sample was characterized by a JEOL JEM-2100 HR-TEM (high-resolution transmission electron microscope), XRD (X-ray

diffraction), EDX (energy-sispersive X-ray), FTIR (infrared spectroscopy), and a Zetasizer (nano 90 Malvern Panalytical, Malvern, UK).

2.3. In Vitro Studies

2.3.1. Antibacterial Activity

Disc Diffusion Method

The antibacterial activities of the γ-Al_2O_3 nanoparticles were evaluated against different extensively drug-resistant (XDR) bacterial strains of *Acinetobacter baumannii*, which were identified and provided from the microbiology lab at the Main University Hospital, Alexandria, Egypt. First, 100 µL of freshly prepared 0.5 McFarland bacterial suspensions were swabbed over the surface of Müeller–Hinton agar (MHA) plates. The disc diffusion method was primarily used to assess the antibacterial activity of the prepared γ-Al_2O_3 nanoparticles (20 mg) [21,22].

Minimum Inhibitory Concentration (MIC)

The MIC test was conducted using a serial dilution technique with the prepared γ-Al_2O_3 nanoparticles. First, 20 µL of tween 80, 80 µL of sterile Müeller–Hinton broth (MHB), and 100 µL of γ-Al_2O_3 nanoparticles were mixed and serially diluted in a 96-well microtiter plate. Then, 100 µl of the freshly prepared 0.5 McFarland bacterial suspensions was inoculated in each well. The MIC is the lowest concentration of the tested nanoparticles to inhibit bacterial growth [21,22].

Bacterial Lethality Curve

The optimal time required for γ-Al_2O_3 nanoparticles to inhibit bacterial growth was assessed through bacterial lethality curve plotting. The determined MIC was incubated with 1 mL of 0.5 McFarland bacterial suspension. Then, at different incubation times (0, 2, 4, 6, 8, 12, and 24 h), aliquots from each tube were taken to assess the bacterial growth using the OD at 600 nm [22].

2.3.2. Al_2O_3 Nanoparticle Mechanistic Action

Transmission Electron Microscope (TEM) Study

A transmission electron microscopic (TEM) examination (JEM-100 CX, JOEL, Shanghai, China) was used to assess the ultrastructures of the bacterial cells after treatment with the MIC of the prepared nanoparticles. TEM has a resolution of 3 nm at 30 kV. Ultrathin sections were prepared on grids then stained with 3% uranyl acetate [23].

Reactive Oxygen Species (ROS) and Double-Strand Break Measurements

Reactive oxygen species (ROS) generation was measured using 2,7-dichlorofluorescin diacetate (DCFH-DA) dye. Using this technique, the extracellular ROS were compared between the control and nanoparticle-treated bacterial cells according to Bhuvaneshwari et al. [24]. Moreover, a DNA strand break assay was performed to quantify the genotoxicity of the prepared nanoparticles against the tested bacteria, following the method described by Bhuvaneshwari et al. [24].

2.3.3. Evaluation of the Cytotoxic Effects of the Prepared γ-Al_2O_3

One of the most vulnerable body parts to *Acinetobacter baumannii* infection is the lung. Hence, a human lung fibroblast (WI-38 cells) normal cell line (ATCC® number: CCL-75™) was chosen to assess the cytotoxicity of the prepared γ-Al_2O_3. The cytotoxic effects were evaluated using an MTT essay, which is a quantitative method to measure the cells' viability after incubation with the tested nanoparticles. Eight serially diluted concentrations of the tested nanoparticles were incubated with a precultured cell line (5×10^4 cell/well) for 24 h. The relation between the living cells and the nanoparticle concentration was plotted using Origin Pro 6.8 software (OriginLab Co., Northampton, MA, USA) to calculate the

survival curve and the cytotoxic concentration (CC50) of the WI-38 cells [25,26] according to Equation (2):

$$\text{Cell Viability\%} = \frac{\text{Treated cells OD}}{\text{Untreated cells OD}} \times 100 \quad (2)$$

3. Results and Discussion

3.1. Preparation and Characterization of the Nanoyields

After the cathodic plasma process, deionized water was ionized in reactive oxygen, hydrogen, and hydroxide species, which interacted with Al ion clusters to produce γ-Al_2O_3. The prepared nanosample was examined using an HR-TEM study. The results showed that the Al_2O_3 was a mix of rod and spherical shapes in the nano range with diameters of less than 30 nm (Figure 1a). It was important to investigate the corresponding nanoparticle yield [27]. The powder XRD pattern of the sample was used to obtain information about the surface plane (Figure 1b). The pattern assigned to the intensities of the peaks revealed the presence of nano-γ-aluminum oxide, as JCPDS No. 29–0063, with prominent peaks at 2θ values of 37.1°, 45.76°, and 66.79°, corresponding to primitive cubic class values (h, k, and l) of 311, 400, and 440, respectively [28]. The XRD data and HR-TEM results confirmed that the samples were pure and without impurities. Γ-Al_2O_3 were crystalline materials. The EDX analysis proved the purity (100%) of the prepared nanoparticles of γ-Al_2O_3 (Figure 1e). The average crystallite size of the obtained pure Al_2O_3 was calculated to be 3.45 nm using Debye Scherer's method (Table 1).

Table 1. Size distribution calculations.

(2Θ) Degree	Intensity (Counts)	(h, k, and l) MillerIndices	FWHM Degree	Grain Size (nm)
35.91	78.21	(311)	8.73	1.00
45.73	102.34	(400)	1.93	4.67
66.79	111.69	(440)	2.13	4.67

The crystallinity index was evaluated through the equation expressed as:

$$\mathrm{I_{cry}} = \frac{D_{p(TEM)}}{D_{cry(XRD)}} \quad (3)$$

where $\mathrm{I_{cry}}$ is the crystallinity index; D_p is the particle size (obtained from the HRTEM morphological analysis); and D_{cry} is the particle size (calculated from the Scherrer equation). The crystallinity index displayed a score higher than 1.0, which indicated that the prepared yield was polycrystalline.

The FTIR spectrum of γ-alumina showed a broad band at 3465 cm^{-1} attributed to the -OH stretching vibrations related to the lattice of water molecules; this may indicate the presence of moisture in the powder. In addition, the available bands at 1637, 1153, and 1072 cm^{-1} were the consequence of symmetrical bending vibrations of the Al–O–H group. There was a weak band due to Al-O bond vibration at 1332 cm^{-1} and symmetric bending stretching vibration of Al-O-Al at 701 cm^{-1} (Figure 1d). The same observations were reported by Wasan et al. [29]. The double regular peaks observed between 2979 cm^{-1} and 2886 cm^{-1} indicated the small drops of HCl added to the sample during the preparation process [30].

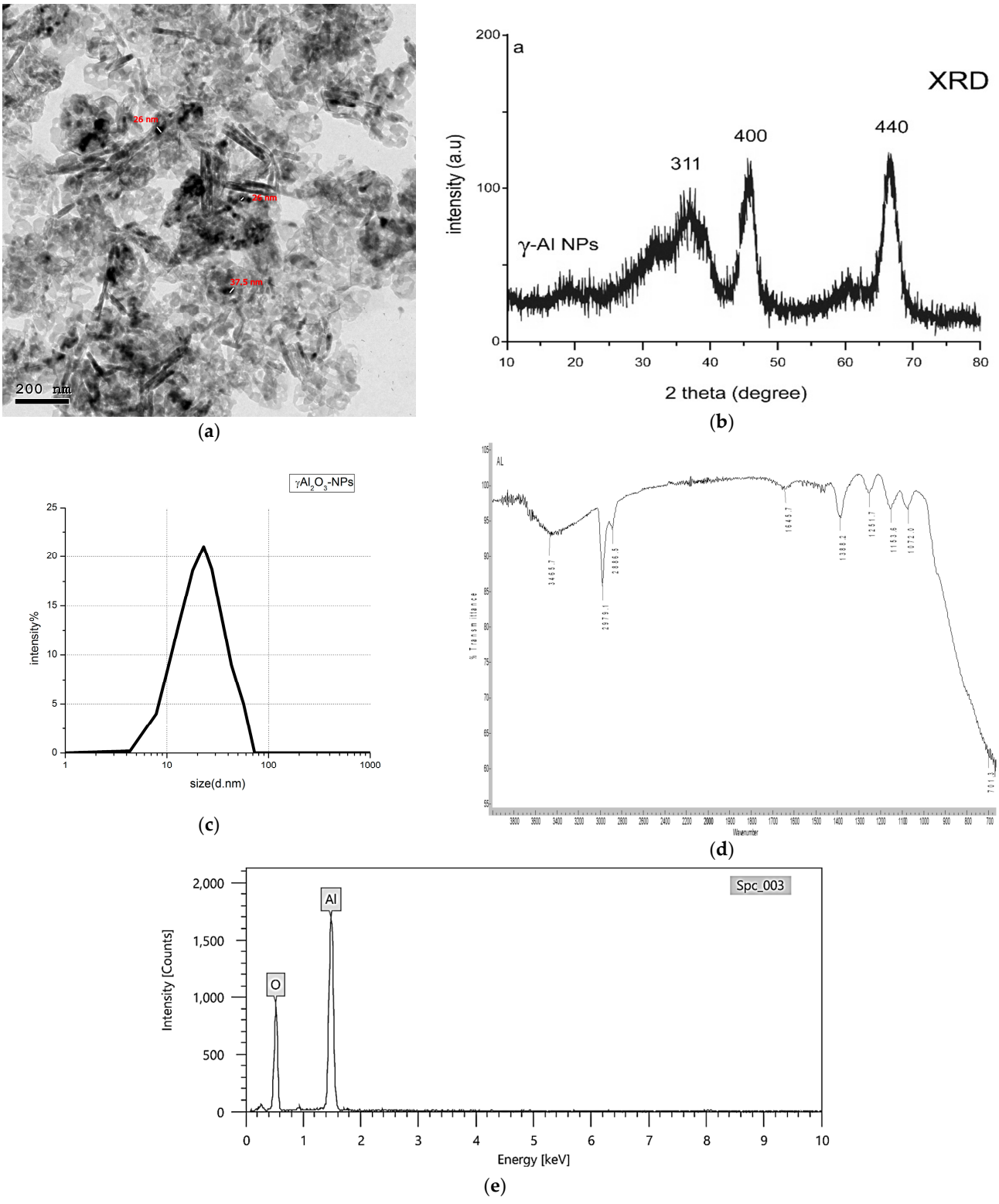

Figure 1. Physicochemical characterization of the synthesized γ-Al_2O_3, including (**a**) TEM, (**b**) XRD pattern, (**c**) particle size, (**d**) FTIR spectroscopy, and (**e**) EDX studies of the synthesized nanoparticles.

When electrodes were immersed in dielectric media, an applied strong electric field was sufficient to break down the barrier gap between the aluminum electrodes. As a result, a huge number of charged electrons were eliminated from the electrode-created aluminum ions. The vaporized aluminum ions interfaced with the liquid to condense

it as a bottom-up method into its stabilized nanosized form. The zeta potential was determined to estimate the surface charge for γ-Al_2O_3 (−34 ± 1.8 mV), which indicates the good stability of the produced nanoparticles [28]. As shown in Figure 1c, the full width at half-maxima of γ-Al_2O_3 fluctuated nearly to its peak position, which indicated the non-homogenous size distribution of the produced yield. One can conclude that strong applied fields must be provided with enough energy to remove the electron from an electrode and separate aluminum ions in deionized water to properly create the arc plasma between the cathode/anode gap. The difference between the energy required and the work function for the electrons' removal may be transferred as heat energy in the solution or may play a significant role in changing the produced ions' crystal order (changing the resultant shapes) [28].

3.2. In Vitro Studies

3.2.1. Antibacterial Activity

The results presented in Table 2 proved the promising antibacterial activity of the prepared nanoparticles. The most susceptible strain was *A. baumannii* strain 3, with an inhibition zone diameter that reached 19 mm and an MIC value that reached 2 mg/mL. *A. baumannii* strain 3 was chosen for further investigations. The data in Figure 2 showed a significant reduction in the bacterial growth after a 12 h incubation with aluminum oxide nanoparticles. This result provided an additional advantage for aluminum oxide nanoparticles to completely eradicate the bacterial growth in a short time. The antibacterial activity of Al_2O_3 nanoparticles was previously tested against several pathogens, namely *Staphylococcus aureus*, *Streptococcus mutans*, *Escherichia coli*, and *Proteus vulgaris*. The results presented the promising antibacterial activity of the prepared nanoparticles due to the nanoparticles' large surface area [31]. Jwad et al. [32] tested the antibacterial activity of aluminum oxide nanoparticles (10-60 nm diameter size), and it was represented by inhibition zone diameters that reached 25.55 mm against *S. aureus* and 20.56 and 19.33 mm against *E. coli* and *P. aeruginosa*, respectively.

Table 2. Antibacterial activity of aluminum oxide nanoparticles.

Tested Strains	**γ-Al_2O_3 NPs**	
	IZ (mm)	**MIC (mg/mL)**
A. baumannii 1	15	8
A. baumannii 2	10	16
A. baumannii 3	19	2
A. baumannii 4	15	8
A. baumannii 5	6	64
A. baumannii 6	13	16
A. baumannii 7	6	64
A. baumannii 8	10	16
A. baumannii 9	7	64
A. baumannii 10	17	8

IZ: inhibition zone diameter, MIC: minimum inhibitory concentration.

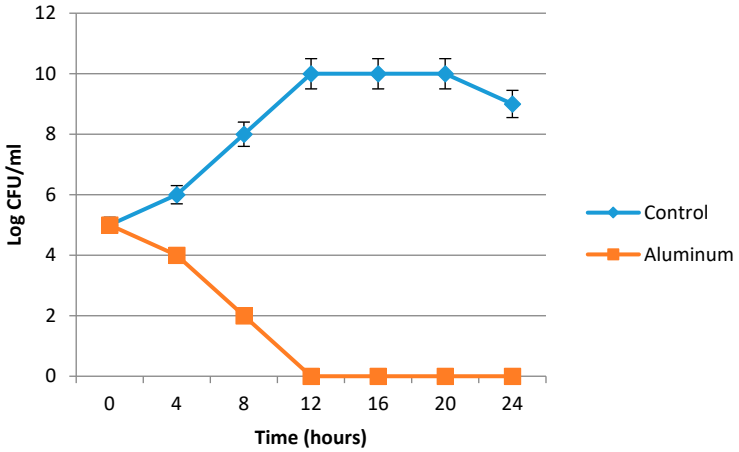

Figure 2. Lethality curve of *A. baumannii* upon treatment with γ-Al_2O_3 NPs.

3.2.2. γ-Al_2O_3 Nanoparticle Mechanistic Action

Several techniques were used to determine the γ-Al_2O_3 nanoparticle mechanism of action against the tested bacteria. A TEM study of the bacteria-treated cells revealed the complete distortion of the bacterial cells and leakage of the intracellular components (Figure 3a). Furthermore, oxidative stress was investigated. The bacterial cell response to interactions with γ-Al_2O_3 nanoparticles usually resulted in a reactive oxygen species (ROS) increment. It was observed that by increasing the nanoparticle concentration from 0.25 to 1.25 mg/mL the ROS content increased by almost 32% (Figure 3b). The Al^{3+} ions released by Al_2O_3 NPs produced ROS, which in turn caused membrane damage and a cell viability reduction. Internalization and γ-Al_2O_3 nanoparticle attachment can potentially harm cell organelles, such as the nucleus (genomic DNA and plasmids) [33].

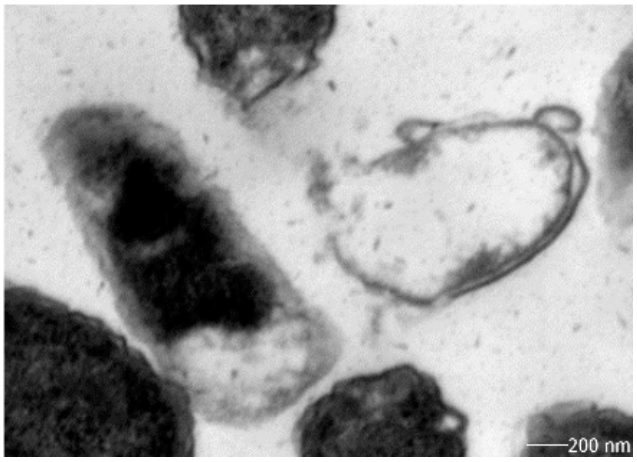

(**a**)

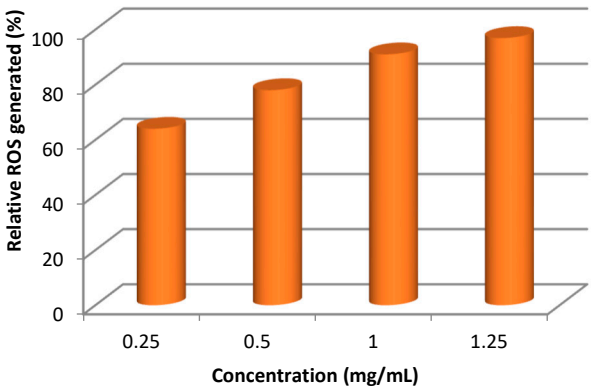

(**b**)

Figure 3. Mechanistic action of the prepared γ-Al_2O_3, analyzed using a TEM study (**a**) and relative ROS generation (**b**).

The genotoxic effect of the prepared nanoparticles was investigated by assessing the rate at which a double-stranded DNA (dsDNA) transited to single-stranded DNA (ssDNA), which was directly proportional to the number of breaks in the phosphodiester backbone. *A. baumannii* cells treated with Al_2O_3 nanoparticles (0.25, 0.5, and 1 mg/L) exhibited significant ($p < 0.05$) DNA damage, with F values of 19.3 ± 0.4, 52.7 ± 0.2, and 75.1 ± 0.6%, respectively. Bhuvaneshwari et al. [24] compared the genotoxic effect of bulk

and nano-Al_2O_3 and reported that Al_2O_3 nanoparticles showed more potent effects on Gram-negative bacteria than Gram-positive bacteria. DNA damage can cause cell apoptosis or necrosis by triggering signal transduction pathways, leading to cell death [24].

3.3. Cytotoxic Effects of the Prepared Nanoparticles

In a trial to study the in vitro cytotoxic effects of the prepared γ-Al_2O_3-NPs, the cell proliferation using a normal human lung fibroblast cell line (WI-38 cells) was tested. A lung fibroblast cell line was chosen due to the possible biomedical application of the prepared γ-Al_2O_3-NPs as a potent treatment against *Acinetobacter baumannii* infection. It was found that the CC50 of γ-Al_2O_3-NPs was 1250 µg/mL (Figure 4).

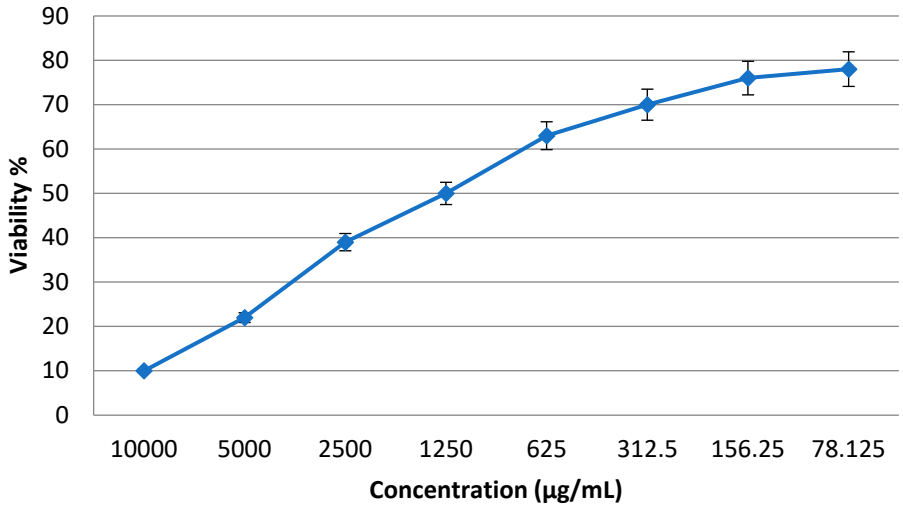

Figure 4. The cytotoxic effect of the prepared γ-Al_2O_3-NPs.

4. Conclusions

γ-Al_2O_3-NPs were successfully synthesized on a nano scale using an arc discharge method. Clearly, the structure phase of γ-Al_2O_3 and its size influenced the bacterial inhibition activity. In summary, γ-Al_2O_3 had a diameter less than 30 nm and a zeta potential of -34 ± 1.8 mV. In vitro studies were applied to assess the antibacterial activity of the prepared nanoparticles, focusing on their mechanistic action. γ-Al_2O_3 nanoparticles inhibited bacterial growth by disrupting the bacterial cell membrane and inducing ROS. The CC50 of the prepared γ-Al_2O_3-NPs was 1250 µg/mL in a normal human lung fibroblast cell line (WI-38 cells). According to the high antibacterial activity, the prepared nanoparticles can be considered as potent saviors in the combat against extensive resistant nosocomial strains.

Author Contributions: Conceptualization, B.H.E. and M.E.-K.; methodology, B.H.E. and M.E.-K.; software, M.E.-K. and A.M.E.; validation, B.H.E.; formal analysis, M.E.-K.; investigation, A.R.Z.A., A.M.A., H.E.-K., and A.M.E.; writing—original draft preparation, A.R.Z.A., A.M.A., H.E.-K., and A.M.E.; writing—review and editing, B.H.E. and M.E.-K. All authors have read and agreed to the published version of the manuscript.

Funding: This research received no external funding.

Institutional Review Board Statement: Not applicable.

Informed Consent Statement: Not applicable.

Data Availability Statement: Not applicable.

Conflicts of Interest: The authors declare no conflict of interest.

References

1. Luis, A.I.S.; Campos, E.V.R.; de Oliveira, J.L.; Fraceto, L.F. Trends in aquaculture sciences: From now to use of nanotechnology for disease control. *Rev. Aquac.* **2019**, *11*, 119–132. [CrossRef]
2. Adlhart, C.; Verran, J.; Azevedo, N.F.; Olmez, H.; Keinänen-Toivola, M.M.; Gouveia, I.; Melo, L.F.; Crijns, F. Surface modifications for antimicrobial effects in the healthcare setting: A critical overview. *J. Hosp. Infect.* **2018**, *99*, 239–249. [CrossRef] [PubMed]
3. Al-Humaidi, J.Y.; Hagar, M.; Bakr, B.A.; Elwakil, B.H.; Moneer, E.A.; El-Khatib, M. Decorative Multi-Walled Carbon Nanotubes by ZnO: Synthesis, Characterization, and Potent Anti-Toxoplasmosis Activity. *Metals* **2022**, *12*, 1246. [CrossRef]
4. Aljohani, F.S.; Elsafi, M.; Ghoneim, N.I.; Toderaş, M.; Sayyed, M.I.; Mohafez, H.; Islam, M.A.; Khandaker, M.U.; El-Khatib, M. Water Treatment from MB Using Zn-Ag MWCNT Synthesized by Double Arc Discharge. *Materials* **2021**, *14*, 7205. [CrossRef] [PubMed]
5. Iijima, S. Helical microtubules of graphitic carbon. *Nature* **1991**, *354*, 56–58. [CrossRef]
6. Arora, N.; Sharma, N. Arc discharge synthesis of carbon nanotubes: Comprehensive review. *Diam. Relat. Mater.* **2014**, *50*, 135–150. [CrossRef]
7. El-Khatib, A.M.; El-khatib, M. Synthesis of hexagonal nanozinc by arc discharge for antibacterial water treatment. *Surf. Innov.* **2020**, *8*, 165–171. [CrossRef]
8. El-Khatib, A.; Khalil, A.; Ismail, M.; Elkhatib, M. The combined effects of multisized silver nanoparticles and pulsed magnetic field on K. pneumonia. *Bioinspired Biomim. Nanobiomater.* **2019**, *8*, 154–160. [CrossRef]
9. Baghdadi, A.M.; Saddiq, A.A.; Aissa, A.; Algamal, Y.; Khalil, N.M. Structural refinement and antimicrobial activity of aluminum oxide nanoparticles. *J. Ceram. Soc. Jpn.* **2022**, *130*, 257–263. [CrossRef]
10. Jiao, Z.; Liu, Z.; Zhao, X. Cathode-arc-anode behavior in cooling-induced cathode-focusing GTA system: A unified numerical model. *Int. J. Heat Mass Transf.* **2022**, *199*, 123484. [CrossRef]
11. Li, W.F.; Ma, X.L.; Zhang, W.S.; Zhang, W.; Li, Y.; Zhang, Z.D. Synthesis and characterization of γ-Al_2O_3 nanorods. *Phys. Status Solidi* **2006**, *203*, 294–299. [CrossRef]
12. Delaportas, D.; Svarnas, P.; Alexandrou, I.; Siokou, A.; Black, K.; Bradley, J.W. γ-Al_2O_3 nanoparticle production by arc-discharge in water: In situ discharge characterization and nanoparticle investigation. *J. Phys. D Appl. Phys.* **2009**, *42*, 245204. [CrossRef]
13. Humphries, R.M.; Kircher, S.; Ferrell, A.; Krause, K.M.; Malherbe, R.; Hsiung, A.; Burnham, C.-A.D. The Continued Value of Disk Diffusion for Assessing Antimicrobial Susceptibility in Clinical Laboratories: Report from the Clinical and Laboratory Standards Institute Methods Development and Standardization Working Group. *J. Clin. Microbiol.* **2018**, *56*, e00437-18. [CrossRef] [PubMed]
14. Halbus, A.F.; Horozov, T.S.; Paunov, V.N. Colloid particle formulations for antimicrobial applications. *Adv. Colloid Interface Sci.* **2017**, *249*, 134–148. [CrossRef] [PubMed]
15. Boucher, H.W.; Talbot, G.H.; Bradley, J.S.; Edwards, J.E.; Gilbert, D.; Rice, L.B.; Scheld, M.; Spellberg, B.; Bartlett, J. Bad Bugs, No Drugs: No ESKAPE! An Update from the Infectious Diseases Society of America. *Clin. Infect. Dis.* **2009**, *48*, 1–12. [CrossRef] [PubMed]
16. Arias, C.A.; Murray, B.E. Antibiotic-Resistant Bugs in the 21st Century—A Clinical Super-Challenge. *N. Engl. J. Med.* **2009**, *360*, 439–443. [CrossRef] [PubMed]
17. Magiorakos, A.-P.; Srinivasan, A.; Carey, R.B.; Carmeli, Y.; Falagas, M.E.; Giske, C.G.; Harbarth, S.; Hindler, J.F.; Kahlmeter, G.; Olsson-Liljequist, B.; et al. Multidrug-resistant, extensively drug-resistant and pandrug-resistant bacteria: An international expert proposal for interim standard definitions for acquired resistance. *Clin. Microbiol. Infect.* **2012**, *18*, 268–281. [CrossRef]
18. Basak, S.; Singh, P.; Rajurkar, M. Multidrug Resistant and Extensively Drug Resistant Bacteria: A Study. *J. Pathog.* **2016**, *2016*, 4065603. [CrossRef] [PubMed]
19. El-Khatib, A.M.; Elsafi, M.; Sayyed, M.; Abbas, M.; El-Khatib, M. Impact of micro and nano aluminium on the efficiency of photon detectors. *Results Phys.* **2021**, *30*, 104908. [CrossRef]
20. Sulaiman, S.; Mahmud, A.A.A.; Bakar, M.H.A.; Noor, A.Z.M. Aluminum Nanoparticles Preparation via Plasma Arc Discharge. In *Progress in Engineering Technology III*; Advanced Structured, Materials; Abu Bakar, M.H., Nurhidayat Zahelem, M., Öchsner, A., Eds.; Springer: Cham, Switzerland, 2021; Volume 148. [CrossRef]
21. Elnaggar, Y.S.; Elwakil, B.H.; Elshewemi, S.S.; El-Naggar, M.Y.; A Bekhit, A.; A Olama, Z. Novel Siwa propolis and colistin-integrated chitosan nanoparticles: Elaboration; in vitro and in vivo appraisal. *Nanomedicine* **2020**, *15*, 1269–1284. [CrossRef]
22. Aljohani, F.S.; Hamed, M.T.; Bakr, B.A.; Shahin, Y.H.; Abu-Serie, M.M.; Awaad, A.K.; El-Kady, H.; Elwakil, B.H. In vivo biodistribution and acute toxicity evaluation of greenly synthesized ultra-small gold nanoparticles with different biological activities. *Sci. Rep.* **2022**, *12*, 6269. [CrossRef] [PubMed]
23. Dorgham, R.A.; Abd Al Moaty, M.N.; Chong, K.P.; Elwakil, B.H. Molasses-Silver Nanoparticles: Synthesis, Optimization, Characterization, and Antibiofilm Activity. *Int. J. Mol. Sci.* **2022**, *23*, 10243. [CrossRef] [PubMed]
24. Bhuvaneshwari, M.; Bairoliya, S.; Parashar, A.; Chandrasekaran, N.; Mukherjee, A. Differential toxicity of Al2O3 particles on Gram-positive and Gram-negative sediment bacterial isolates from freshwater. *Environ. Sci. Pollut. Res.* **2016**, *23*, 12095–12106. [CrossRef] [PubMed]
25. Elwakil, B.H.; Toderas, M.; El-Khatib, M. Arc discharge rapid synthesis of engineered copper oxides nano shapes with potent antibacterial activity against multi-drug resistant bacteria. *Sci. Rep.* **2022**, *12*, 20209. [CrossRef] [PubMed]
26. El-Shaer, H.; Elwakil, B.H.; Bakr, B.A.; Eldrieny, A.M.; El-Khatib, M.; Chong, K.P.; Gazia, A.A.A. Physiotherapeutic Protocol and ZnO Nanoparticles: A Combined Novel Treatment Program against Bacterial Pyomyositis. *Biology* **2022**, *11*, 1393. [CrossRef]
27. Bell, T.E.; González-Carballo, J.M.; Tooze, R.P.; Torrente-Murciano, L. Single-step synthesis of nanostructured γ-alumina with solvent reusability to maximise yield and morphological purity. *J. Mater. Chem. A* **2015**, *3*, 6196–6201. [CrossRef]

28. Wang, J.; Zhao, D.; Zhou, G.; Zhang, C.; Zhang, P.; Hou, X. Synthesis of nano-sized γ-Al_2O_3 with controllable size by simple homogeneous precipitation method. *Mater. Lett.* **2020**, *279*, 128476. [CrossRef]
29. Al-Rubayee, W.T.; Abdul-Rasheed, O.F.; Ali, N.M. Preparation of a Modified Nanoalumina Sorbent for the Removal of Alizarin Yellow R and Methylene Blue Dyes from Aqueous Solutions. *J. Chem.* **2016**, *2016*, 4683859. [CrossRef]
30. Zemek, P.; Van Gompel, J.; Plowman, S. PPM-Level HCl Measurements from Cement Kilns and Waste Incinerators by FTIR Spectroscopy. MIDAC Corporation. Available online: http://www.midac.com/files/AP-212.pdf (accessed on 22 November 2022).
31. Geoprincy, G.; Gandhi, N.N.; Renganathan, S. Novel antibacterial effects of alumina nanoparticles on *Bacillus cereus* and *Bacillus subtilis* in comparison with antibiotics. *Int. J. Pharm. Pharm. Sci.* **2012**, *4*, 544–548.
32. Jwad, K.H.; Saleh, T.H.; Abd-Alhamza, B. Preparation of Aluminum Oxide Nanoparticles by Laser Ablation and a Study of Their Applications as Antibacterial and Wounds Healing Agent. *Nano Biomed. Eng.* **2019**, *11*, 313–319. [CrossRef]
33. Pakrashi, S.; Kumar, D.; Iswarya, V.; Bhuvaneshwari, M.; Chandrasekaran, N.; Mukherjee, A. A comparative ecotoxicity analysis of α- and γ-phase aluminium oxide nanoparticles towards a freshwater bacterial isolate *Bacillus licheniformis*. *Bioprocess Biosyst. Eng.* **2014**, *37*, 2415–2423. [CrossRef] [PubMed]